Hierarchical Upscaling of Data-Driven Damage Diagnostics for Stiffened Composite Aircraft Structures

Agnes Broer[1,2(✉)], Nan Yue[1,2], Georgios Galanopoulos[3], Rinze Benedictus[1], Theodoros Loutas[3], and Dimitrios Zarouchas[1,2]

[1] Structural Integrity and Composites Group, Faculty of Aerospace Engineering, Delft University of Technology, Kluyverweg 1, 2629HS Delft, The Netherlands
a.a.r.broer@tudelft.nl

[2] Center of Excellence in Artificial Intelligence for Structures, Faculty of Aerospace Engineering, Delft University of Technology, Kluyverweg 1, 2629HS Delft, The Netherlands

[3] Laboratory of Applied Mechanics and Vibrations, Department of Mechanical Engineering and Aeronautics, University of Patras, 26500 Rio, Greece

Abstract. To move towards a condition-based maintenance practice for aircraft structures, design of reliable health management methodologies is required. Development of diagnostic methodologies is commonly realised on simplified sample structures with assumptions that methodologies can be adapted for application to realistic aircraft structures under in-service conditions. Yet such actual applications are not conducted. In this work, we study the development of diagnostic methodologies to training structures and their application to dissimilar testing structures. A heterogeneous population is considered, consisting of single-stiffener composite panels for methodology development and training and a multi-stiffener composite panel for application and testing. Characteristics as its composite material, lay-up, and temperature condition are constant while topologies and applied loads differ between the dissimilar structures. Damage in the structural panels is monitored on multiple diagnostic levels using a variety of structural health monitoring (SHM) techniques, including acoustic emission and distributed strain sensing. Specifically, we develop diagnostic methods for localising and monitoring disbond growth after impact using strain data collected during fatigue testing of multiple single-stiffener panels and apply these for disbond monitoring in an upscaled version of a multi-stiffener panel. In this manner, this study aids in the maturement and application of SHM methodologies to realistic aircraft structures.

Keywords: Aircraft · Composite structures · Damage diagnostics · Population · Upscaling

1 Introduction

The implementation of condition-based maintenance (CBM) practices in the aircraft industry may result in lower costs by reducing unnecessary maintenance actions. This is achieved by early damage detection, enhanced maintenance planning and prognostics,

P. Rizzo and A. Milazzo (Eds.): EWSHM 2022, LNCE 254, pp. 975–984, 2023.
https://doi.org/10.1007/978-3-031-07258-1_98

and scaling down unnecessary inspections and preventive replacements. CBM for aircraft structures requires permanently installed sensing systems to allow implementing structural health monitoring (SHM), thereby providing information on damage and degradation processes while the aircraft is in-service. In recent years, various SHM methodologies for different damage diagnostic purposes and using different SHM techniques have been developed for composite structures [1–3].

Researchers often develop such methodologies using data collected during test campaigns conducted in laboratories in which simplified structures or coupons are tested under simplified loading conditions. Yet composite structures installed in aircraft are complex sub-components containing various assembly details, curvatures, and consisting of multiple sub-elements, which are subjected to varying fatigue loads and environmental conditions. The application of the developed diagnostic methodologies from the generic laboratory elements on such sub-component structures is not currently regarded in literature and its performance and validity are thus unclear. Yet for in-service applications, such studies are required for a safe implementation of SHM. Solutions such as testing a similarly large number of subcomponent structures under various conditions, as is commonly done in research projects for generic elements, is not viable due to high costs and limited facilities.

Instead, approaches must be promoted in which methods are developed and trained on generic elements, for which many diverse tests can be performed, and that can be applied to realistic structures, for which little tests and data is available. In this manner, heterogeneous populations can be constructed in which data and knowledge can be exchanged between distinct structures for the purpose of SHM [4]. In future operational stages, this may even be expanded during in-service application by exchanging datasets between various aircraft and their structures, thereby creating a larger heterogeneous population and, with that, larger datasets and a transfer of knowledge between dissimilar structures, resulting in population-based SHM [4, 5].

In this work, the first steps are taken towards the implementation of a hierarchical approach towards damage diagnostics for composite aircraft structures. The application of a diagnostic method for disbond growth monitoring, developed on generic composite elements (single-stiffener panel), to a higher-level composite structure (multi-stiffener panel) is presented. Distributed strain data is collected using optical fibre sensors during hierarchical experimental test campaigns in which the panels are subjected to fatigue compression after impact (FCAI) tests. A disbond growth identification and localisation methodology has been developed using strain data obtained solely from the single-stiffener panels [6]. Considering the single- and multi-stiffener panels as hierarchical structures, the applicability of such methodology by direct consideration on the multi-stiffener panel is evaluated.

2 Experimental Campaign on Heterogeneous Population

A hierarchical test campaign was performed as part of the H2020 ReMAP[1] project[2] on stiffened composite aerospace structures [5, 7]. Damage monitoring in the panels

[1] Real-time condition-based maintenance for adaptive aircraft maintenance planning (ReMAP).
[2] https://h2020-remap.eu/.

has been performed using various SHM techniques that include, among others, acoustic emission, Lamb waves, fibre optic sensing (both fibre Bragg gratings and Rayleigh-backscattering distributed strain sensing), and vibration-based sensing. Two distinct structures are considered in the heterogeneous population: 1) single-stiffener skin panels and 2) multi-stiffener skin panels, displayed in Fig. 1. The single-stiffener skin panels are generic elements consisting of a single T-stiffener and skin while the multi-stiffener panels are sub-components consisting of five T-stiffeners and a skin. The hierarchical structures have various identical characteristics including material, lay-up, and manufacturing procedure; namely, carbon fibre-reinforced epoxy (IM7/8552), a skin lay-up of $[45/\text{-}45/0/45/90/\text{-}45/0]_S$, and a stiffener lay-up of $[45/\text{-}45/0/45/\text{-}45]_S$. The topology of the two structures diverges in terms of number of stiffener elements and dimensions. Namely, where the single-stiffener panel contains one T-stiffener, the multi-stiffener panel contains five T-stiffeners. In essence, the multi-stiffener panel can be seen as a scaled-up version of the single-stiffener panel, with dimensions of its free skin area of 865 × 1030 mm versus 165 × 240 mm, respectively. Note that the dimensions of the T-stiffeners in both lateral (x) and out-of-plane (z) direction are consistent among the distinct structures.

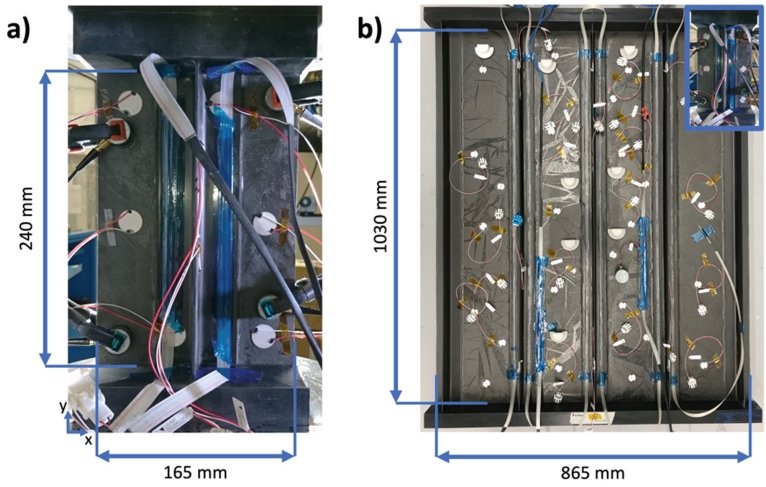

Fig. 1. Hierarchical composite structures sensorised with various SHM techniques: a) single-stiffener panel, b) multi-stiffener panel, adapted from [8].

As indicated, the general heterogeneous population consists of both single- and multi-stiffener panels. Note that in this work, the application of the diagnostic methodology to only one multi-stiffener panel is considered, based on the diagnostic methodology development using nine single-stiffener panels. All structures are subjected to FCAI tests with the fatigue loading consisting of sinusoidal compression-compression (C-C) loads for both structures. Other aspects of the loading conditions differ, such as impact energy, load levels, and frequency, whose details are provided in Table 1. Lastly, it must be noted that the generic single-stiffener panels have been subjected to fatigue loads until a loss in load-bearing capacity was observed, while the fatigue test on the multi-stiffener

panel was stopped after approximately 1,046 $\times$ 10^3 cycles, after which a quasi-static residual strength test until failure was performed.

Table 1. Details on testing aspects for each of the distinct panels.

Testing characteristics	Single-stiffener panels	Multi-stiffener panel
Type of test	FCAI	FCAI
Fatigue loading	C-C	C-C
Stress ratio	10	10
Frequency	2 Hz	1 Hz
Minimum load level	−6.5 kN	Constant amplitude block loading: varying min and max load levels in the range [−10, −230] kN
Maximum load level	−65.0 kN	
Cycles to failure	Varying: minimum of 66 $\times$ 10^3 cycles maximum of 756 $\times$ 10^3 cycles	1,046 $\times$ 10^3 cycles followed by a residual strength test
Number of impacts	1	4
Impact(s) after # cycles	5,000 cycles	42,084 cycles
Impact energy	10 J	1) 15.2 J, 2) 19.8 J, 3) 15.2 J, 4) 17.2 J
Impact locations	8 on stiffener foot 1 on skin	3 on stiffener foot 1 on skin

During fatigue testing, distributed strain data is recorded every 500 and 1000 cycles during a quasi-static loading segment for the single- and multi-stiffener panel, respectively, using an optical fibre and a LUNA Optical Distributed Sensor Interrogator (ODiSI-B) with an acquisition rate of 23.8 Hz, a spatial resolution of 0.65 mm, and a sampling rate of 1 Hz. The quasi-static loading segment ranges from the minimum to the maximum compressive fatigue load and in this study the strain measurement at maximum compressive load is utilised. A SMARTape optical fibre [9] is employed for strain measurements, which is adhesively bonded using cyanoacrylate to the surface of the stiffener feet. For the single-stiffener panel, a centre region of 140 mm is monitored, while for the multi-stiffener panel, the centre three stiffeners are monitored over a central length of 830 mm.

3 Methodology

3.1 Disbond Growth in Single-Stiffener Panels

Optical fibre strain data can be employed for diagnostic purposes such as disbond growth monitoring under fatigue loads by virtue of changing strain distributions under disbond presence. Due to the applied compressive loads, the panels are in a post-buckled state at the time of strain recording and a single half-wave is observed for the single-stiffener panel. The presence of a disbond at the skin-stiffener bondline in the considered single-stiffener panels has a different effect on surface strain values recorded using the SMARTapes, dependent on the direction of out-of-plane deflection under buckling, as shown

in Fig. 2 [6]. The exposed effects of the disbond presence on the strain distribution have been adopted to develop a diagnostic method for disbond growth localisation and monitoring, of which details are outlined in Broer et al. [6] for three single-stiffener panels. The validity of the method has been confirmed on an additional 6 single-stiffener panels [5].

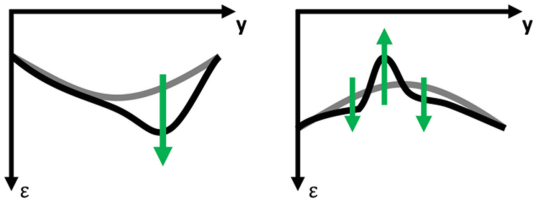

Fig. 2. Graphical representation of the effect of disbond presence on the surface strain of the stiffener foot dependent on the out-of-plane deflection, adapted from [6]. The black line indicates the presence of a disbond and the grey line indicates no disbond presence.

The disbond growth identification and localisation method is a windowing-based approach in which the strain measurement at a given acquisition time is split into a spatial window w_s of $w_s = 5$ measurements (equalling an approximate length of 3.25 mm). Strain measurements of the windows are compared over consecutive cycle measurements and an absolute threshold θ of $\theta = 2\sigma$ is set to detect a change in strain measurements. Here, σ is defined as the arithmetic mean of the window variances for the given window. If the change in strain is in the applicable direction (dependent on the out-of-plane deflection at the given side) and is identified for $w_c = 2000$ cycles, where w_c is the set window of consecutive acquisition cycles, it is stated that disbond growth is occurring at the given location along the stiffener foot.

3.2 Application of Diagnostic Methodology in Multi-stiffener Panel

In the hierarchical upscaling approach of this work, not only disbond growth monitoring in single-stiffener panels is of interest, but also that in the multi-stiffener panel. The knowledge gained on skin-stiffener disbond growth in single-stiffener panels can be employed for such a purpose. It is expected that, given a similar material, lay-up, and manufacturing procedure, equal effects of the disbond on surface strains in the multi-stiffener panels will be observed. Consequently, this implies that the developed methodology for disbond growth identification and localisation can be applied for damage diagnostics on the multi-stiffener panel, thereby allowing for a transfer of knowledge without the need for starting from scratch in the development of disbond monitoring methods.

Initial testing on a multi-stiffener panel reveals a disparity in half-waves between the distinct panels, with a single half-wave for the single-stiffener panel (Fig. 2) and six half-waves for the multi-stiffener panel. This implies that the patterns of disbond presence, which for the single-stiffener panel differ per side, are now present along the length of a single stiffener foot. As an opposite effect in strain changes was observed (an increase versus a decrease) for the different directions of out-of-plane deflection

in the single-stiffener panel, a segmentation step is implemented for the strain data of each stiffener foot in the multi-stiffener panel to ensure that, for a given segment, the appropriate examination is performed.

In its implementation on the multi-stiffener panel, the disbond growth localisation and identification method requires the setting of three parameters, namely w_c, w_s, and θ. The strain measurement interval increased from 500 to 1000 cycles for the multi-stiffener panel, causing w_c to increase to $w_c = 4000$ cycles. Moreover, w_s is set to $w_s = 3$ measurements with an approximate window length of 1.95 mm. Lastly, θ is set similar as for the single-stiffener panel at $\theta = 2\sigma$.

4 Results and Discussion

In the FCAI tests of the single-stiffener panels, it was observed that the damage created by an impact is not directly detrimental to the load-bearing capacity of the panel. However, when positioned at the stiffener feet, a consecutive skin-stiffener disbond may grow under the applied fatigue loads, leading to a larger effect on the global performance and the end-of-life of the panel. In the FCAI test of the multi-stiffener panel, a similar behaviour was foreseen and observed in which the panel preserves its load-bearing capacity after impact. To identify subsequent disbond growth under the applied fatigue loads, the disbond growth monitoring and localisation approach developed on the single-stiffener panels was implemented for damage diagnostics of the multi-stiffener panel, providing results for the centre three stiffener feet along a centre length of 830 mm.

As outlined in Sect. 2, the multi-stiffener panel was impacted four times after 42,084 cycles, and its location with respect to the stiffener feet is summarised in Table 2. Each impact is situated in a region of strain measurement, in other words, at the feet of one of the three centre stiffeners, except for impact 4, which is an impact in the skin region adjacent to the right foot of stiffener 2.

Table 2. Details of impacts performed on the multi-stiffener panels with left and right foot as seen from the stiffener-side and locations (x, y) following the axis defined in Fig. 1.

Impact number	Stiffener	Left or right foot	x [mm]	y [mm]
1	4	Left foot	612	795
2	3	Right foot	465	800
3	3	Left foot	410	660
4	2	Skin next to right foot	285	645

The disbond monitoring method provides six outcomes, one for each monitored stiffener foot, and which are displayed in Fig. 3a) to f) for stiffener foot 2–left to stiffener foot 4–right, respectively. Each figure shows the change in strain for a given location along the stiffener foot (y-axis) and a given cycle number (x-axis) with respect to the initial strain measurement at the start of the experimental campaign. At two given instances, a disbond growth is localised in the multi-stiffener panel. Firstly, a disbond growth is

identified in the left foot of stiffener two at 954 $\times$ 10^3 cycles and y = 382 mm (Fig. 3a). Secondly, a short period of disbond growth is observed in the left foot of stiffener three at 630 $\times$ 10^3 cycles and y = 660 mm (Fig. 3c). The first instance of identified disbond growth is not neighbouring any impact, giving room to the hypothesis that a new disbond may have formed in this location. The second instance corresponds to the location of impact 3, which is located at (x, y) = (410, 660) mm on the left foot of stiffener three. Hence, it is likely that this identified disbond growth is originating from the original impact damage.

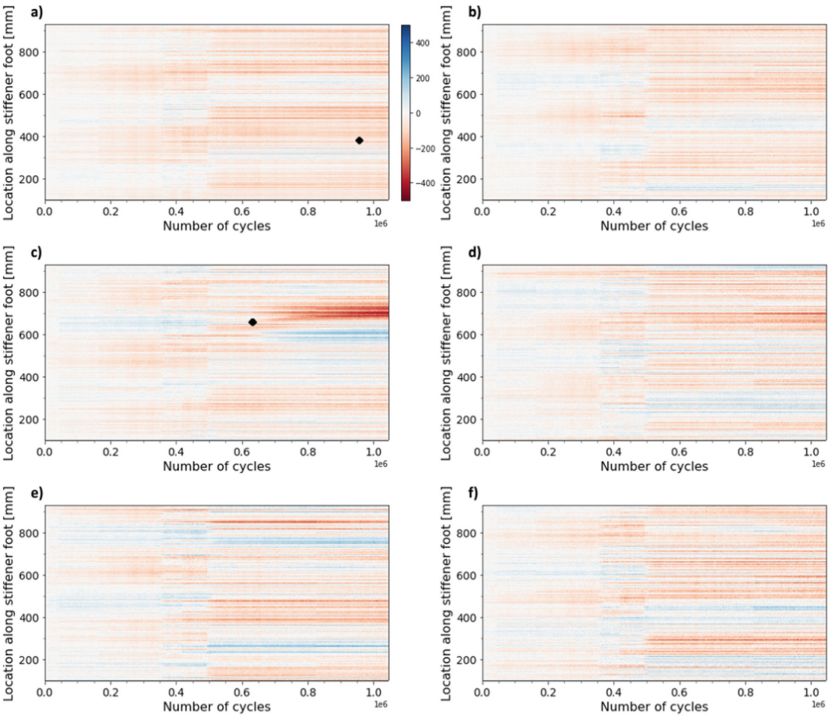

Fig. 3. Disbond growth monitoring results for the multi-stiffener panel for stiffener foot. a) 2–left, b) 2–right, c) 3–left, d) 3–right, e) 4–left, f) 4–right. Colours indicate the change in microstrain with respect to the initial measurement before the start of the fatigue test; colourbar of a) is applicable to all sub-figures. Black diamonds indicate the detection and estimated location of a disbond growth.

To test both hypotheses and to validate the disbond growth identification results, phased array ultrasound images collected using a handheld C-scan device are employed. Throughout the test campaign, frequent images were gathered at various cycle instances to identify damage initiation and propagation along the stiffeners of the multi-stiffener panels. For impact 3, a disbond growth was observed between 506 $\times$ 10^3 and 666 $\times$ 10^3 cycles, and a slower but present disbond growth after 666 $\times$ 10^3 cycles, as presented in Fig. 4. For the remaining three impacts, no disbond growth was witnessed throughout the fatigue test. Additionally, the non-impacted stiffener regions were monitored during

the fatigue test, and no new areas of damage growth were found using the phased array ultrasonic inspection technique.

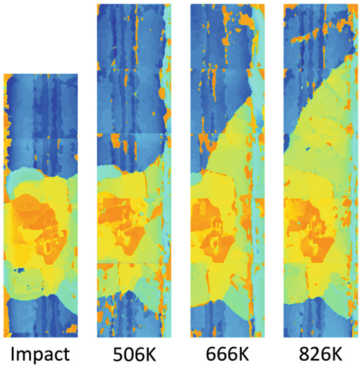

Fig. 4. Phased array images of impact 3 at various fatigue cycles.

When correlating the two found instances of disbond growth based on distributed strain data to the phased array image results, the first instance located at the second stiffener may be considered as an invalid detection. Several hypotheses can be argued on the discrepancy between the two techniques, including the presence of actual damage growth that is within the noise region of the phased array images leading to an undetected damage presence, or disbonding of the SMARTape causing invalid strain measurements rather than indicating the presence of a skin-stiffener disbond. To confirm either, further data analysis with additional SHM techniques is required.

For the second instance of disbond growth identified by the disbond growth monitoring model, both the phased array image results and the strain-based results comply with one another. It is evident that the disbond growth detected by the model at 630×10^3 cycles in the left foot of stiffener three is a disbond growth originating from the original impact damage. Notable is the subsequent identified disbond growth using the phased array images after 666×10^3 cycles, not indicated by the model, which is likely due to its slow propagation speed causing the changes in strain to be below the noise levels and thereby remaining undetected. This is further confirmed by the continued change in strain level as indicated by the increased intensity of the colours in Fig. 3c. Nonetheless, given the successful identification of disbond growth at the earlier stage, it is expected that with suitable modifications in the user-set parameters, disbond growth can be identified in the multi-stiffener panels.

5 Conclusions

A hierarchical upscaling approach for damage diagnostics was presented on the topic of disbond growth monitoring using strain measurements for stiffened aircraft structures. A heterogeneous population was constructed consisting of both single- and multi-stiffener composite panels. A method for disbond growth identification and localisation under fatigue loading was developed using data collected during FCAI tests on generic single-stiffener panels. Based on similar characteristics between the distinct panels, including material, lay-up, and manufacturing procedure, it was demonstrated that the knowledge gained regarding disbond growth and its effects on the measured surface strain can be transferred to the upscaled multi-stiffener panel. Thereby allowing for an implementation with minimal adjustments of the method for disbond growth identification and localisation in the distinct structure, despite differences in topology and loading conditions. As such, benefits are obtained as it displays the possibilities for method development on generic elements and its subsequent application to realistic sub-component structures. In future work, the strain measurement-based study for disbond growth monitoring will be incorporated in a more comprehensive diagnostic framework in which data from multiple SHM techniques is fused for hierarchical upscaling within a heterogeneous population of stiffened composite aircraft structures.

Acknowledgements. We would like to express our gratitude to the ReMAP project partners for their efforts on the experimental campaigns: Embraer, Optimal Structural Solutions, Smartec, Cedrat Technologies, and École Nationale Supérieure d'Arts et Métiers, as well as our colleagues at the laboratories of Delft University of Technology and University of Patras for their technical support. This work was financially supported by the European Union's Horizon 2020 research and innovation program under grant agreement No. 769288.

References

1. Güemes, A., Fernandez-Lopez, A., Pozo, A.R., Sierra-Pérez, J.: Structural health monitoring for advanced composite structures: a review. J. Compos. Sci. **4**(1), 13 (2020). https://doi.org/10.3390/jcs4010013
2. Ricci, F., Monaco, E., Boffa, N.D., Maio, L., Memmolo, V.: Guided waves for structural health monitoring in composites: a review and implementation strategies. Prog. Aerosp. Sci. **129**, 100790 (2020). https://doi.org/10.1016/j.paerosci.2021.100790
3. Saeedifar, M., Zarouchas, D.: Damage characterization of laminated composites using acoustic emission: a review. Compos. Part B: Eng. **195**, 108039 (2020). https://doi.org/10.1016/j.compositesb.2020.108039
4. Worden, K., et al.: A brief introduction to recent developments in population-based structural health monitoring. Front. Built Environ. **6**, 146 (2020). https://doi.org/10.3389/fbuil.2020.00146
5. CORDIS - European Commission Horizon 2020 Project: Real-time condition-based maintenance for adaptive aircraft maintenance planning (ReMAP), grant agreement ID: 769288 (2018). https://cordis.europa.eu/project/id/769288. Accessed 13 Jan 2022
6. Broer, A., Galanopoulos, G., Benedictus, R., Loutas, T., Zarouchas, D.: Fusion-based damage diagnostics for stiffened composite panels. Struct. Health Monit. **21**(2), 613–639 (2022). https://doi.org/10.1177/14759217211007127

7. Zarouchas, D., Broer, A., Galanopoulos, G., Briand, W., Benedictus, R., Loutas, T.: Compression compression fatigue tests on single stiffener aerospace structures. DataverseNL, V1 (2021). https://doi.org/10.34894/QNURER
8. Broer, A.A.R., Yue, N., Galanopoulos, G., Benedictus, R., Loutas, T., Zarouchas, D.: On the challenges of upscaling damage monitoring methodologies for stiffened composite aircraft panels. In: Proceedings of the IWSHM 2021, 13th International Workshop on Structural Health Monitoring (2022)
9. Inaudi, D., Glisic, B.: Development of distributed strain and temperature sensing cables. In: Proceedings of the SPIE 5855, 17th International Conference on Optical Fibre Sensors, vol. 5855, pp. 222–225. SPIE, The International Society for Optics and Photonics, Bellingham, WA (2005)